On possible convective regimes of a subsurface ocean beneath Ganymede's ice shell (conclusions)

Jakub Kvorka[1], Libor Šachl[1]

[1]Charles University in Prague, Faculty of Mathematics and Physics, Department of Geophysics

26.09.2024

Control parameters

Flux-based Rayleigh number, $Ra_q = \frac{1}{4\pi r_o(r_o - D_o)} \frac{\alpha_w g_o Q}{\rho_w C_{p,w} \Omega^3 D^2}$

Ekman number, $Ek = \nu_w / \Omega D_o^2$

Prandtl number, $Pr = \nu_w / \kappa_w$

Estimates based on the model of internal structure

The heat flow Q and ocean thickness D_o can be sourced from Vance et al. [2018] and have been used in numerous studies [e.g., Soderlund, 2019, Terra-Nova et al., 2023, Cabanes et al., 2024].

α_w - thermal expansivity, g_o - grav. acceleration at the outer boundary, ΔT - superadiabatic temperature difference, D_o - thickness of the ocean, ν_w - kinematic viscosity, κ_w - thermal diffusivity, Ω - rotational period

Internal structure of Ganymede

r_o [km]	D_o [km]	D_i [km]	aspect ratio	Ek	Ra_q
2629	518	5	0.80	$6.7{\cdot}10^{-13}$	$1.7{\cdot}10^{-9}$
2608	493	26	0.81	$7.4{\cdot}10^{-13}$	$1.9{\cdot}10^{-9}$
2564	361	70	0.86	$1.4{\cdot}10^{-12}$	$3.5{\cdot}10^{-9}$
2500	119	134	0.95	$1.3{\cdot}10^{-11}$	$3.1{\cdot}10^{-8}$
2478	24	157	0.99	$3.1{\cdot}10^{-10}$	$7.4{\cdot}10^{-7}$

Table: The radius of the ocean outer boundary r_o, the ocean thickness D_o, ice shell thickness D_i and the aspect ratio of the ocean are sourced from Vance et al. [2018]. The radius of Ganymede is fixed at 2634 km and the heat flow, $Q = 470$ GW, is derived from radiogenic heating as described in Hay and Matsuyama [2019]. The Prandtl number value of 10 is based on the molecular values of viscosity and thermal diffusivity [Kvorka and Čadek, 2022]. Values of other quantities involved are obtained from [Soderlund, 2019]: $\nu_w = 1.8{\cdot}10^{-6}\,\mathrm{m^2 s^{-1}}$, $\alpha_w = 2{\cdot}10^{-4}\,\mathrm{K^{-1}}$, $\rho_w = 1150\,\mathrm{kg m^{-3}}$, $\Omega = 10^{-5}\,\mathrm{s^{-1}}$, $C_{p,w} = 3500\,\mathrm{J kg^{-1} K^{-1}}$, $g_o = 1.4\,\mathrm{m s^{-2}}$.

Radius ratio: 0.80

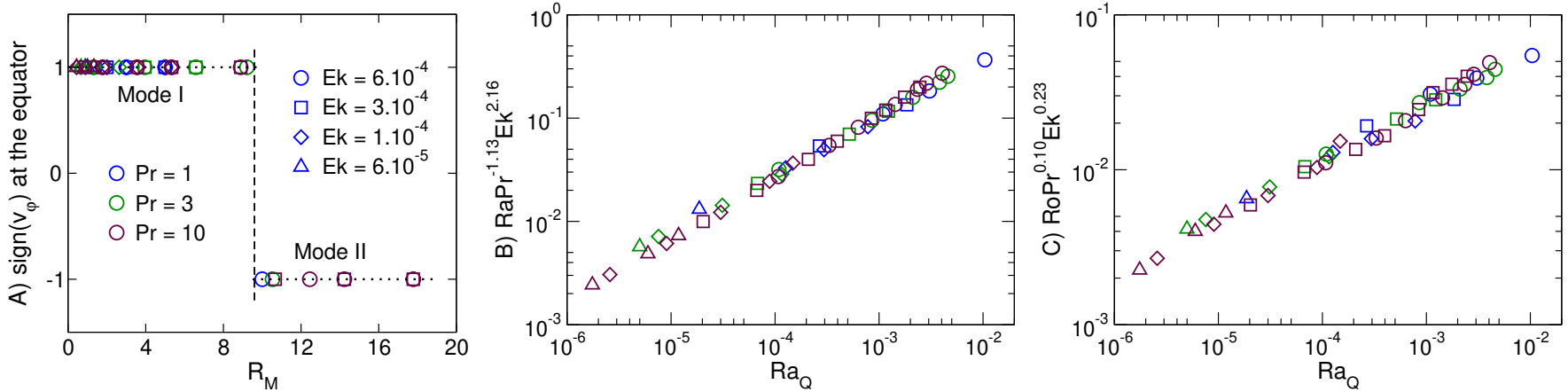

r_o [km]	D [km]	H [km]	Ek	Ra_Q	Ra	U [m/s]
2629	518	5	$6.7{\cdot}10^{-13}$	$1.7{\cdot}10^{-9}$	$1.3{\cdot}10^{23}$	0.49
2608	493	26	$7.4{\cdot}10^{-13}$	$1.9{\cdot}10^{-9}$	$1.1{\cdot}10^{23}$	0.47

Figure: Models of internal structure of Ganymede with aspect ratio close to 0.80 [Vance et al., 2018]. r_o is the outer radius of the ocean, D is the thickness of the ocean and H denotes the thickness of the ice shell. U is dimensional rms velocity derived form the scaling presented in panel C. The ocean is situated in the transitional regime regardless the ocean thickness (D), as $Ro_{loc} \approx 10^3$ and $Ro_c \approx 0.08$ in both cases. The flow geometry resembles Mode II, as $R_M \approx 31$.

Radius ratio: 0.80, results obtained for $Ek = 3 \cdot 10^{-4}$

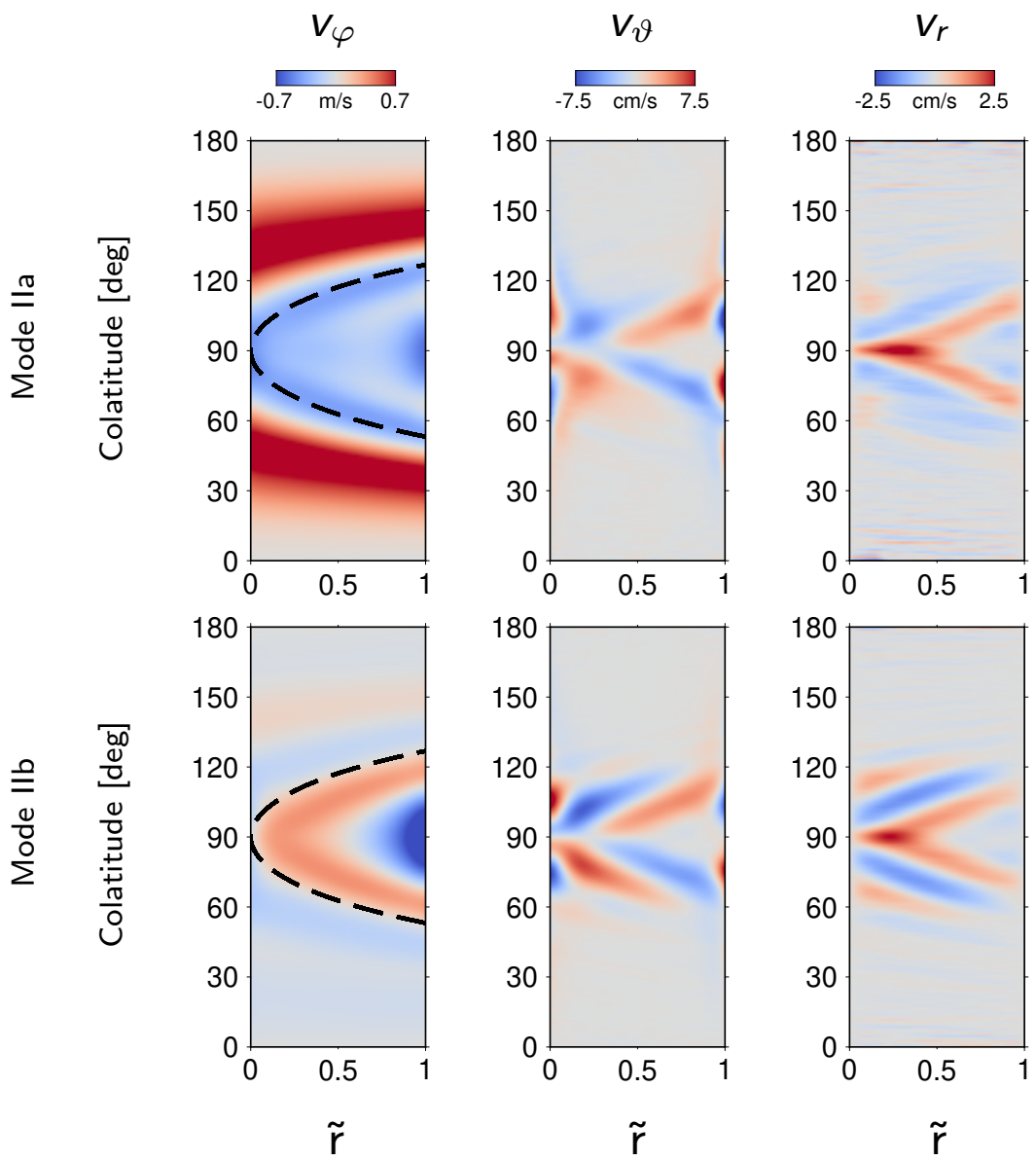

Radius ratio: 0.85

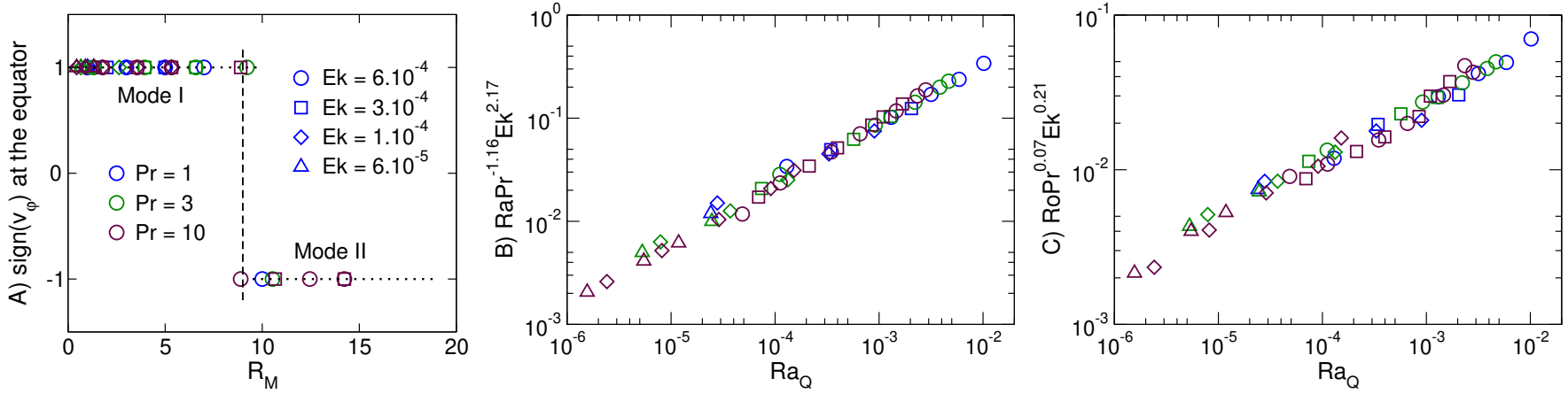

r_o [km]	D [km]	H [km]	Ek	Ra_Q	Ra	U [m/s]
2564	361	70	$1.4{\cdot}10^{-12}$	$3.5{\cdot}10^{-9}$	$4.8{\cdot}10^{22}$	0.21

Figure: Model of internal structure of Ganymede with aspect ratio close to 0.85 Vance et al. [2018]. r_o is the outer radius of the ocean, D is the thickness of the ocean and H denotes the thickness of the ice shell. U is dimensional rms velocity derived form the scaling presented in panel C. The ocean is situated in the transitional regime of convection, as $Ro_{loc} \approx 10^3$ and $Ro_c \approx 0.10$. $R_M \approx 41$ places the ocean into Mode II.

Radius ratio: 0.85, results obtained for $Ek = 6 \cdot 10^{-4}$

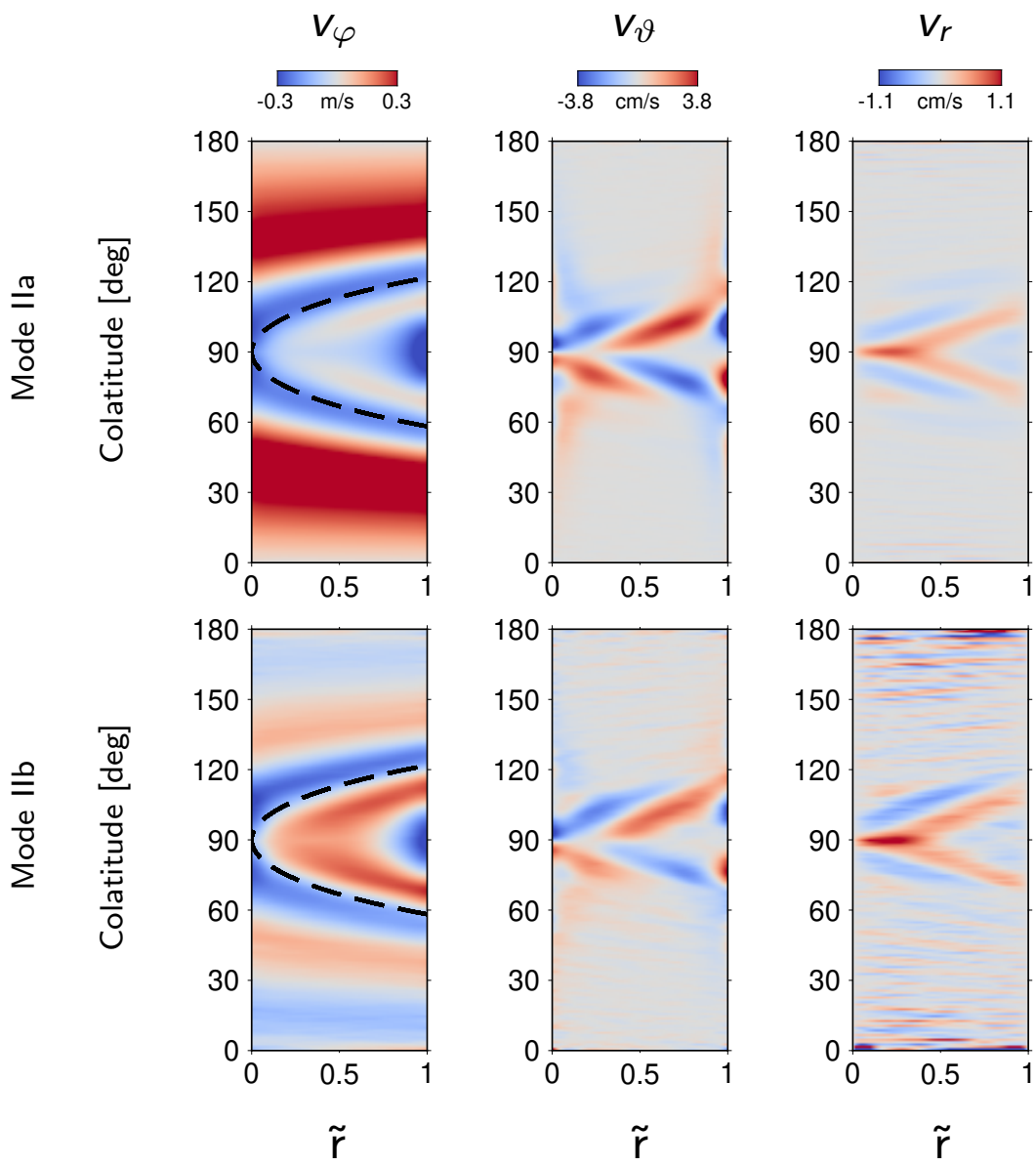

Radius ratio: 0.90 and higher

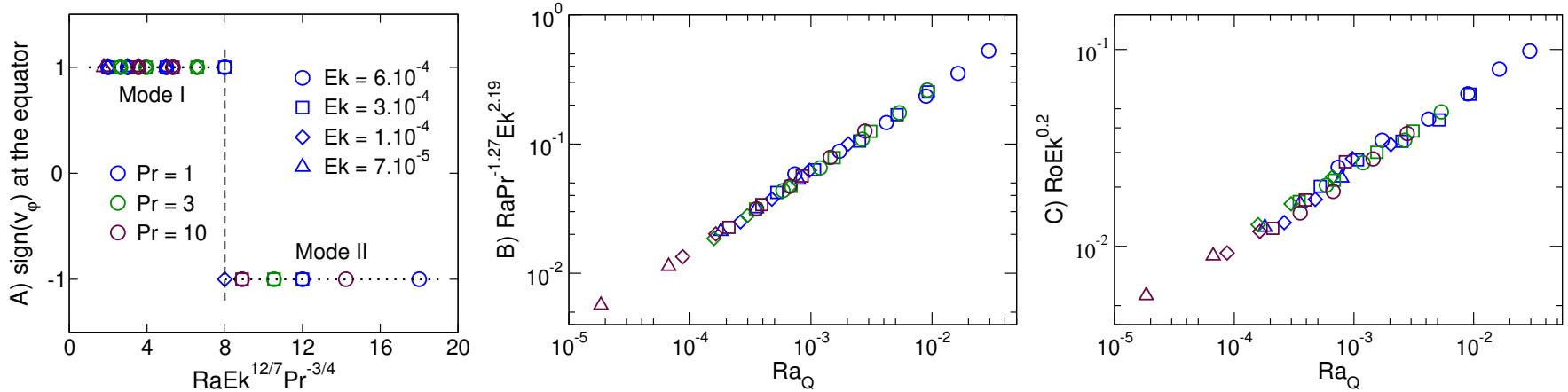

r_o [km]	D [km]	H [km]	Ek	Ra_Q	Ra	U [m/s]
2500	119	134	$1.3{\cdot}10^{-11}$	$3.1{\cdot}10^{-8}$	$1.2{\cdot}10^{21}$	0.08
2477	24	157	$3.1{\cdot}10^{-10}$	$7.4{\cdot}10^{-7}$	$8.3{\cdot}10^{18}$	0.02

Figure: Models of internal structure of Ganymede with aspect ratio 0.90 and higher [Vance et al., 2018]. r_o is the outer radius of the ocean, D is the thickness of the ocean and H denotes the thickness of the ice shell. U is dimensional rms velocity derived form the scaling presented in panel C. The ocean is situated in the transitional regime regardless the ocean thickness (D), as Ro_{loc} exceeds 10^3 and $Ro_c \leq 0.28$ in both cases. The flow geometry resembles Mode II, as $R_M \geq 50$.

Radius ratio: 0.90, results obtained for $Ek = 3 \cdot 10^{-4}$

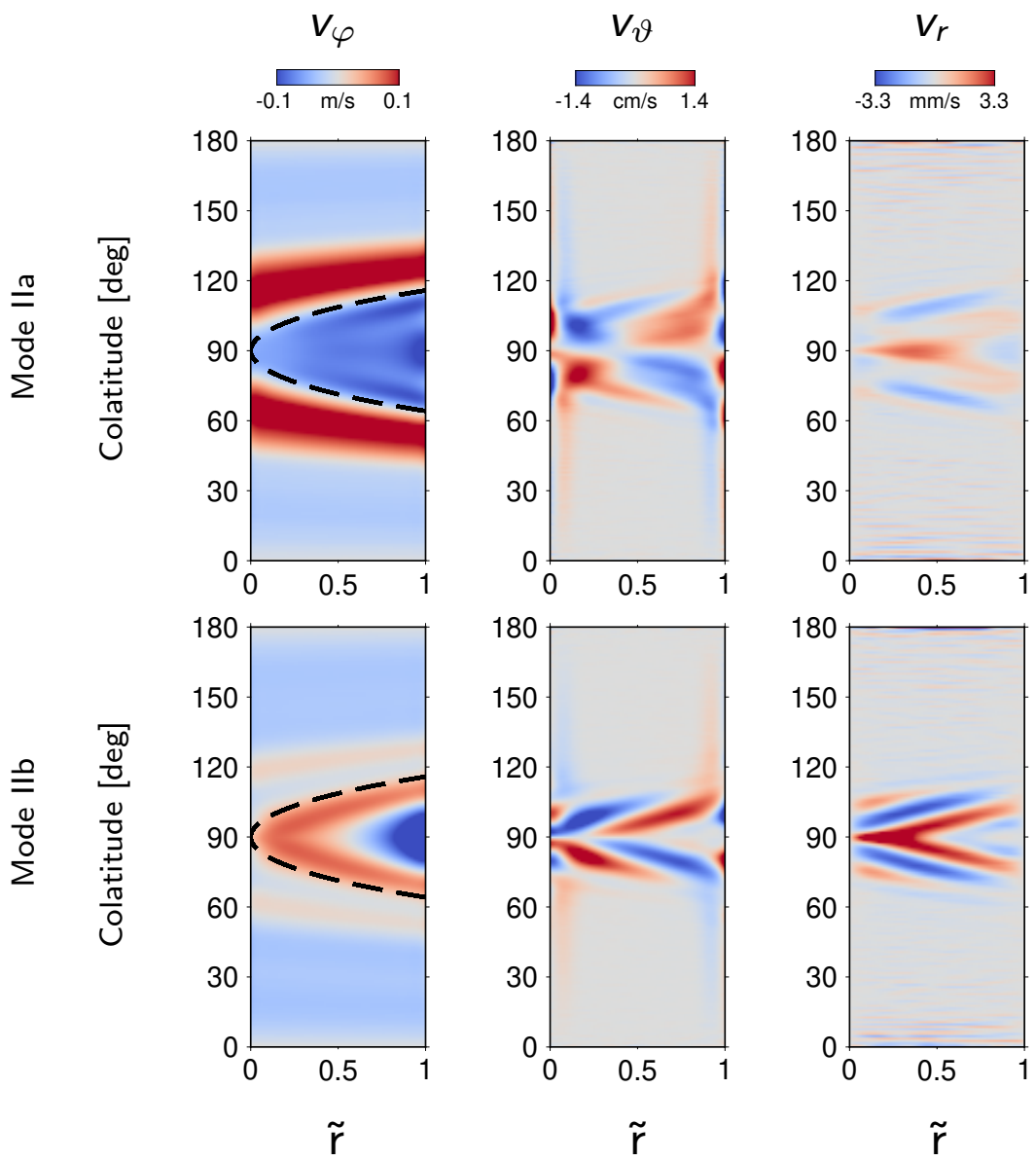

Conclusions

- Dataset covering models of Ganymede ocean thickness is prepared.
- The scaling laws for different thicknesses have been derived: the estimates of the Rayleigh number (10^{19}–10^{23}) are in agreement with the results of Soderlund [2019].
- Results show forking of Mode II into submodes (Mode IIa,b), which differ by zonal jets structure.
- Mode IIa (three jets exceeding outside the tangent cylinder] is a suitable flow pattern for Ganymede's ocean (consistent with Vance et al., 2021).
- Constraints on velocities (tens of cms^{-1}) are consistent with recent suggestions by Cabanes et al. [2024].

References I

S. Cabanes, T. Gastine, and A. Fournier. Zonostrophic turbulence in the subsurface oceans of the Jovian and Saturnian moons. *Icarus*, 415: 116047, 2024. doi: 10.1016/j.icarus.2024.116047.

H.C.F.C. Hay and I. Matsuyama. Nonlinear tidal dissipation in the subsurface oceans of Enceladus and other icy satellites. *Icarus*, 319: 68–85, 2019. doi: 10.1016/j.icarus.2018.09.019.

J. Kvorka and O. Čadek. A numerical model of convective heat transfer in Titan's subsurface ocean. *Icarus*, 376:114853, 2022. doi: 10.1016/j.icarus.2021.114853.

K. M. Soderlund. Ocean dynamics of outer solar system satellites. *Geophys. Res. Lett.*, 46:8700–8710, 2019. doi: 10.1029/2018GL081880.

F. Terra-Nova, H. Amit, G. Choblet, G. Tobie, M. Bouffard, and O. Čadek. The influence of heterogeneous seafloor heat flux on the cooling patterns of Ganymede's and Titan's subsurface oceans. *Icarus*, 389:115232, 2023. doi: 10.1016/j.icarus.2022.115232.

References II

S. D. Vance, M. P. Panning, S. Stähler, F. Cammarano, B. G. Bills, G. Tobie, S. Kamata, S. Kedar, C. Sotin, W. T. Pike, R. Lorenz, H.-H. Huang, J. M. Jackson, and B. Banerdt. Geophysical investigations of habitability in ice-covered ocean worlds. *J. Geophys. Res.: Planets*, 123: 180–205, 2018. doi: 10.1002/2017JE005341.

S. D. Vance, M. J. Styczinski, B. G. Bills, C. J. Cochrane, K. M. Soderlund, N. Gómez-Pérez, and C. Paty. Magnetic induction responses of Jupiter's ocean moons including effects from adiabatic convection. *J. Geophys. Res.: Planets*, 126:e2020JE006418, 2021. doi: doi.org/10.1029/2020JE006418.